УДК 535.3

ИССЛЕДОВАНИЕ ОПТИЧЕСКОЙ АТМОСФЕРНОЙ ТУРБУЛЕНТНОСТИ

Сюань Цянь*, Юнцян Яо, Хуншуан Ван

Национальные астрономические обсерватории Китайской академии наук, Пекин, Китай,
*qianxuan@nao.cas.cn

THE STUDY OF ATMOSPHERIC OPTICAL TURBULENCE

Xuan Qian*, Yongqiang Yao, Hongshuang Wang

National Astronomical Observatory, Chinese Academy of Sciences, Beijing, China,
*qianxuan@nao.cas.cn

Аннотация. При обследовании мест размещения, проектировании и эксплуатации современных крупных телескопов необходимо получать профиль оптической турбулентности атмосферы и оценивать его интегральные параметры. Кроме метода измерения, международное астрономическое сообщество в последние десятилетия разрабатывало методы моделирования оптической турбулентности атмосферы. Мезомасштабная метеорологическая модель используется для получения метеорологических характеристик над выбранной астроплощадкой на основе установленной взаимосвязи между метеорологическими характеристиками и параметрами оптической турбулентности; при этом можно дополнительно рассчитывать параметры оптической турбулентности, такие как C_n^2, качество астрономических изображений (seeing), изопланатический угол, время когерентности и т.д. на основе использования моделей параметризации атмосферной оптической турбулентности. Основываясь на численной модели, мы можем построить систему прогнозирования оптической турбулентности, которая позволит не только обследовать места размещения телескопов по обширной территории, но и станет очень удобным и полезным инструментом для работы существующих обсерваторий и телескопов, а также для изучения характеристик турбулентности. В этой статье, основываясь на предыдущих исследованиях, в краткой форме обсуждаются распределения параметров оптической турбулентности атмосферы по всему Китаю.

Ключевые слова: оптическая турбулентность атмосферы, интенсивность турбулентности C_n^2, качество астрономических изображений, длина когерентности атмосферы, изопланатический угол, время когерентности атмосферы

Abstract. In the site survey, design and operation of modern large telescopes, the atmospheric optical turbulence profile and its integral parameters need to be obtained. In addition to the measurement method, the international astronomical community has gradually developed the model method of atmospheric optical turbulence in recent decades. The mesoscale meteorological model is used to obtain the meteorological parameters at a site, through establishing the relationship between the meteorological parameters and the optical turbulence parameters, the optical turbulence parameters such as C_n^2, seeing, isoplanatic angle, coherence time etc. can be further calculated, that's the model method of atmospheric optical turbulence parameterization. And based on numerical model, the forecast system of optical turbulence can be built, not only for site survey in broad area, but also will be of much convenience and benifits for the operation of observatories and telescopes, as well as the study of turbulence characteristics. In this paper, the distributions of atmospheric optical turbulence parameters all over China are briefly introduced in previous studies.

Keywords: atmospheric optical turbulence, turbulence intensity C_n^2, seeing, atmospheric coherence length, isoplanatic angle, atmospheric coherence time

1. INTRODUCTION

When the light propagates in the atmosphere, the wavefront distortion of the light as well as its intensity flicker will be caused due to the existence of atmospheric optical turbulence. The main parameters describing the effect of turbulence on light are C_n^2, seeing, atmospheric coherence time, isoplanatic angle, and so on. Through the relationship between the meteorological parameters and the optical turbulence intensity C_n^2, the C_n^2 profile and its integral parameters can be calculated, that's the calculation method of atmospheric optical turbulence parameterization model. Using mesoscale numerical meteorological models, as well as the measurement like radiosounding balloon, the distributions of meteorological parameters above an observatory can be obtained. And combined with the turbulence parameterization model, the overall characteristics of optical turbulence above a site, as well as the regional distributions and the prediction of turbulence can be summarized. Since the 1990s, the international astronomical community has gradually developed a method to calculate and forecast the intensity of atmospheric optical turbulence using mesoscale meteorological models ([Bougeault et al., 1995; Masciadri et al., 1999a&b].

In astronomical site survey, the model can be used to find out the optimal area with better optical turbulence conditions, and the work intensity and cost can be greatly reduced, as well as the work efficiency can be improved. Understanding the comprehensive optical turbulence characteristics of observatories can provide necessary parameters for the design and operation of the telescopes. And the prediction of optical turbulence in the local area of the observatory can be used to optimize the observation time of the telescope, and also provide guidance for the best time window of the operation of the ground-based photoelectric equipment. According to the forecast results, the optimal observation path and time can be selected by avoiding the region with strong optical turbulence. In this paper, the regional distributions of atmospheric turbulence parameters all over China are briefly introduced and presented, mainly using the numerical model.

2. METHODS

The meso-scale Weather Research and Forecast numerical model (WRF), is a completely compressible non-statics model, using Arakawa C grid points in the horizontal direction and terrain following mass coordinates in the vertical direction. The third or fourth order Runge-Kutta algorithm is used in time integration. In the confugration of WRF model over the whole China [Wang&Qian, 2012], the time period was the whole 2010, with the horizontal spatial resolution of 30km, and the time interal of 1 hour; meanwhile, in the vertical direction, there were 50 levels covered from ground to the pressure level of 10hPa (about 30km above sea level), with the vertical resolutions range from tens of meters near the ground to nearly 1 km in the upper air. The initial meteorological input data were the FNL (Final Operational Global Analysis) and the GFS (Global Forecast System) data sets, with spatial resolutions of 1°, and the terrain data was the GEOG (Geographical data) with a spatial resolution of 30″.

3. RESULTS

3.1 the structure constant of atmospheric refractive index c_n^2

The C_n^2 indicates the intensity of optical turbulence, its order can approximately predict the effect of atmospheric turbulence on optical link performance, and the effectiveness of prediction depends largely on the configuration of the link and the position of the optical transmitter and receiver. The dependence of each order is the integration of path, and a series of optical turbulence parameters affecting the optical transmission or imaging quality can be obtained by integrating the height. The atmospheric refractive index is a passive conservative quantity, similar to the potential temperature structure constant, and there is a refractive index structure parameter, with which the relation is [Businger et al., 2011; Cherubini et al., 2008],

$$C_n{}^2 = \left(\frac{80*10^{-6}P}{T^2}\right)^2 C_t{}^2 \qquad (1)$$

and the temperature fluctuation structure constant C_t^2 can be determined by the wind shear and the potential temperature gradient,

$$C_t{}^2 = \langle C_t{}^2\rangle_m \frac{\chi}{\langle\chi\rangle_m}\left(\frac{S}{\langle S\rangle_m}\right)^{\frac{1}{2}},$$

$$\chi = \frac{d\theta}{dz}, \quad S = \sqrt{\left(\frac{dV_x}{dz}\right)^2 + \left(\frac{dV_y}{dz}\right)^2},$$

$$\theta = T\left(\frac{1000}{P}\right)^{0.286} \qquad (2)$$

S is the wind shear, χ is the gradient of potential temperature, V_x and V_y are the horizontal and vertical wind speeds, respectively, and $\langle\rangle_m$ indicates the median values of all observations at the same altitude. θ is the potential temperature, T is the temperature and P is the pressure. The potential temperature can be considered as a conserved quantity in the dry adiabatic process, which is defined as the temperature a dry air parcel would have if restored adiabatically from the existing state to a standard pressure of 1000 hPa. In Figure 2 shown the vertical and spatial distributions of C_n^2 above an area or an observatory.

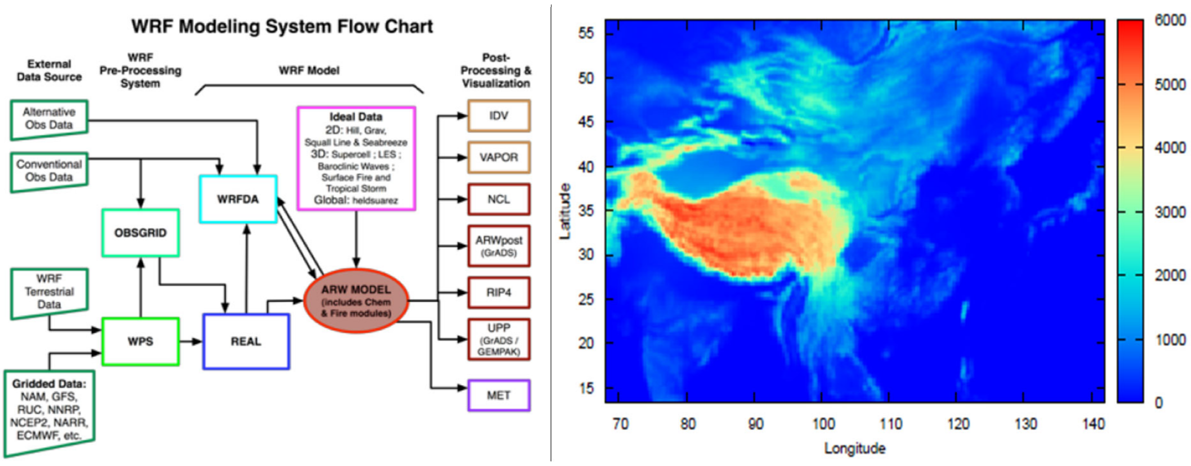

Fig. 1. The flow chart of the WRF model (left), the calculated aera over China using the WRF model (right)

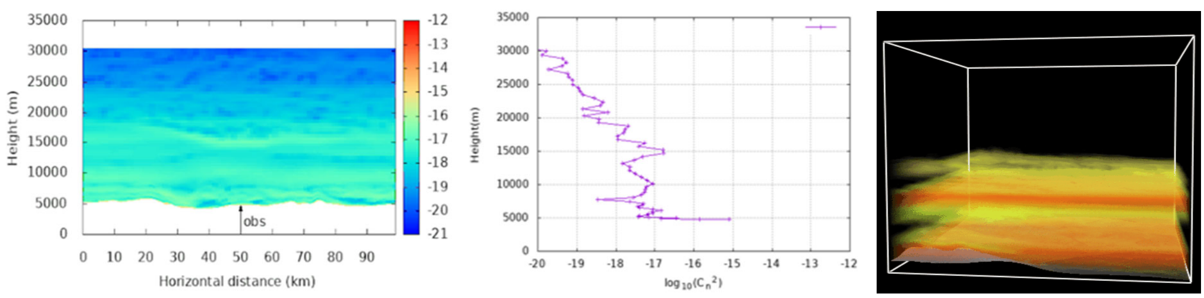

Fig. 2. The vertical distribution of Cn2 slice at E-W direction above an observatory (left), the Cn2 profile at a site (middle), and the spatial distribution of Cn2 (right)

3.2 seeing

The atmospheric seeing represents the full width at half-maximum (FWHM) of the point spread function, the best angular resolution that an optical telescope can achieve in a long exposure image, corresponding to the FWHM of the blurry blob when observing a star through the atmosphere. The seeing ε_0 can be calculated as

$$\varepsilon_0 = 5.25\lambda^{(-1)/5}\left[\int C_n^{\,2}(h)dh\right]^{3/5} \quad (3)$$

λ is the wavelength, p is the total air pressure, h is the altitude and t is the air temperature. At the excellent observatories in the mid-latitude, the typical value of seeing is usually 0.6–1.0 arcsec.

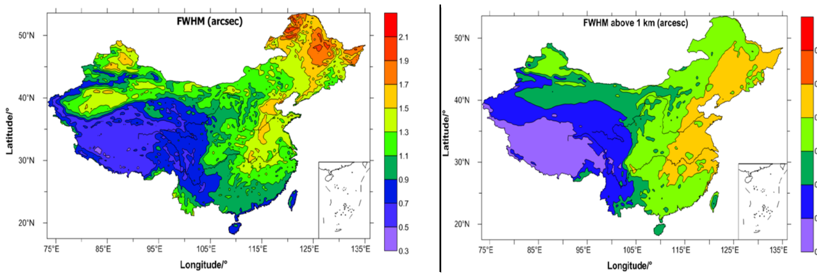

Fig. 3. The distributions of yearly mean seeing in the whole atmosphere (left) and free atmosphere (above 1km, right)

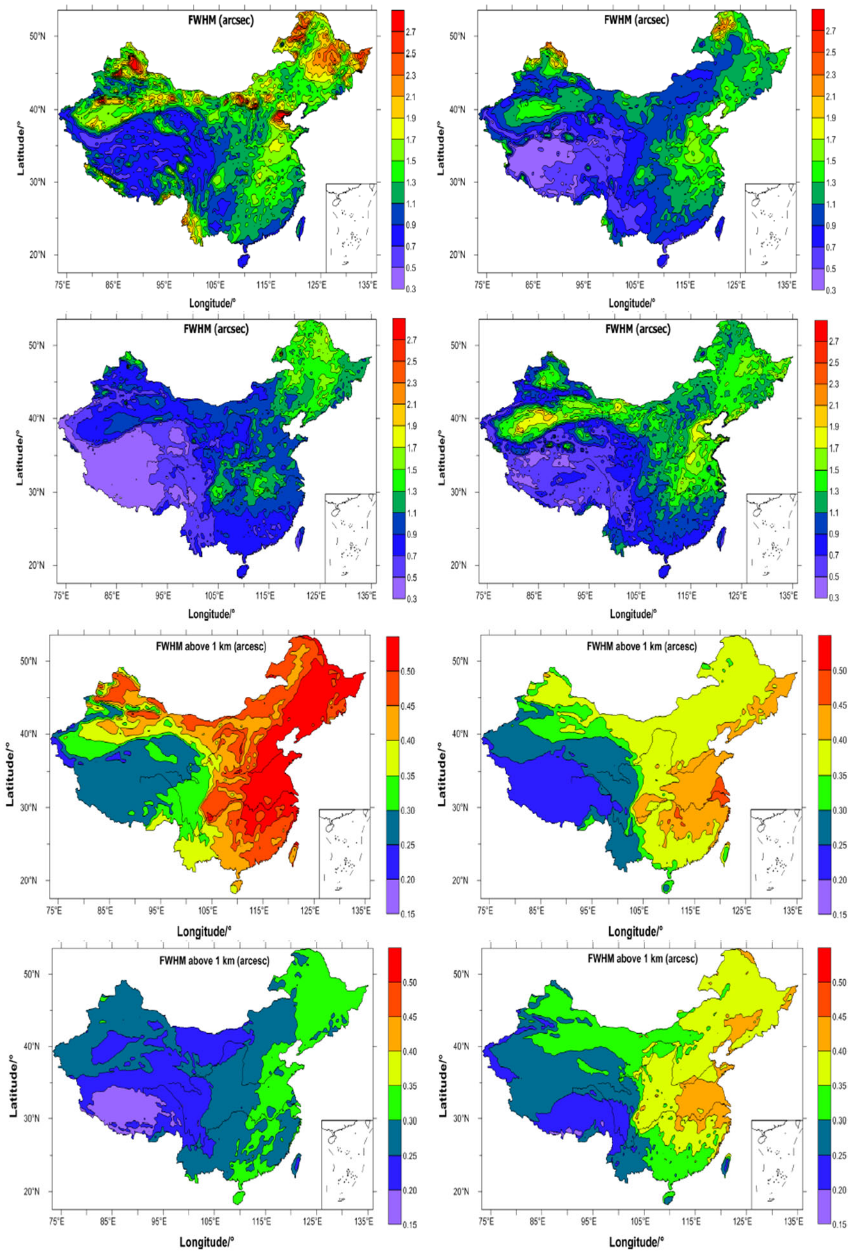

Fig. 4. The seasonal distributions of seeing in the whole atmosphere (top) and free atmosphere (bottom), from left to right are the seeing in January, April, July, and October

3.3 atmospheric coherence time and isoplanatic angle

The atmospheric coherence time τ_0 depends on C_n^2 and the wind speed profiles, while the isoplanatic angle θ_0 accounts on C_n^2, expressed as follows,

$$\tau_0 = 0.058\lambda^{6/5}\left[\int |V(h)|^{5/3} C_n^{\ 2}(h)dh\right]^{(-3)/5}, \quad (4)$$

$$\theta_0 = 0.058\lambda^{6/5}\left[\int h^{5/3} C_n^{\ 2}(h)dh\right]^{(-3)/5} \quad (5)$$

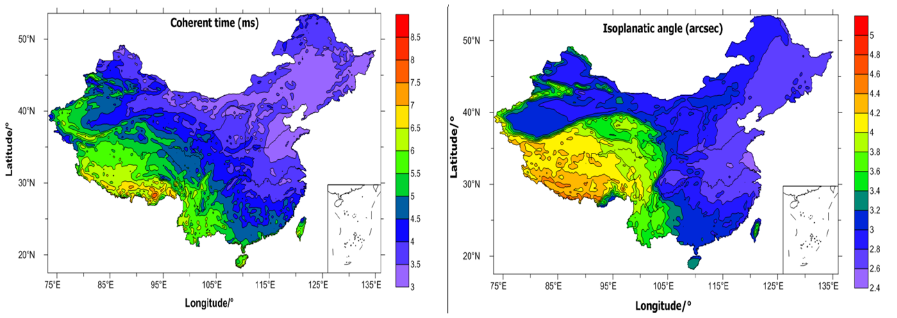

Fig. 5. The distributions of yearly mean atmospheric coherence time (left) and isoplanatic angle (right)

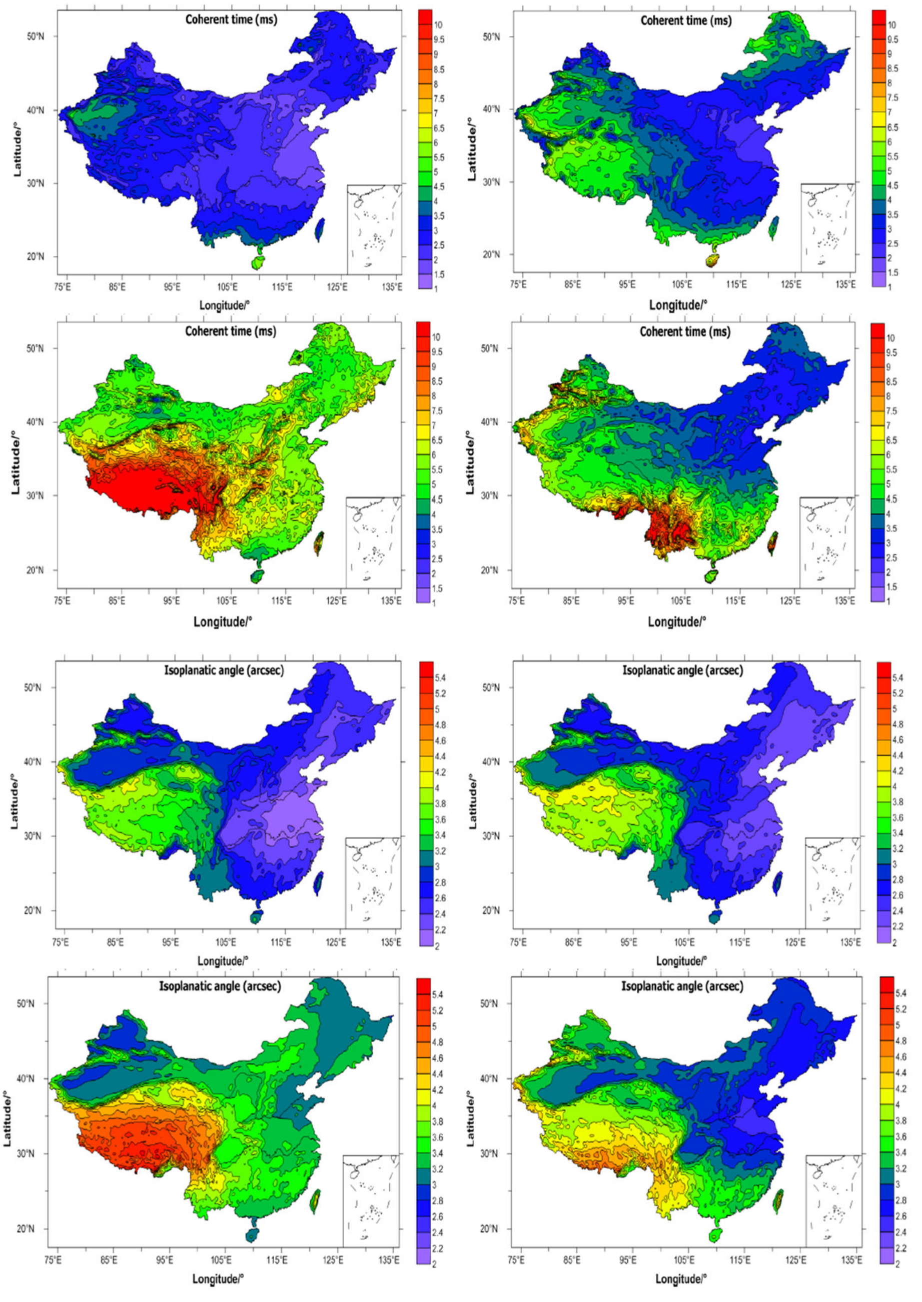

Fig. 6. The seasonal distributions of atmospheric coherence time (top) and isoplanatic angle (bottom), from left to right are the seeing in January, April, July, and October

Furthermore, the intensity and height of high-altitude optical turbulence will significantly affect the θ_0 and τ_0. From Formulas 4–5, the weights of $H^{5/3}$ and $V^{5/3}$ are added in the integrals of C_n^2, respectively. In order to intuitively understand the influence of high altitude turbulence on the θ_0 and τ_0, the vertical profiles of the $C_n^2H^{5/3}$ and the $C_n^2\ V^{5/3}$ are presented in Figure 7. In the near-ground layer, that has little effect on the θ_0 where much influencing the seeing value, and the $C_n^2H^{5/3}$ in the upper air is obviously higher than that in near-ground layer. The $C_n^2V^{5/3}$ both in near-ground layer and in upper air vary little, while the thickness in the upper air is greater than that near the ground, and the influence of the upper air on the τ_0 is much greater than that of the ground layer.

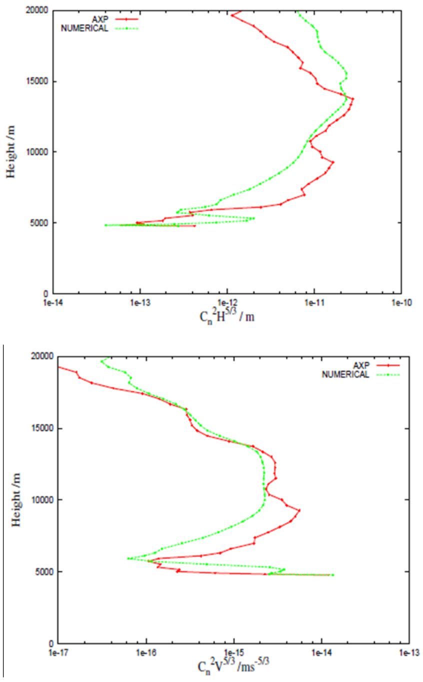

Figure 7 The mean $C_n^2H^{5/3}$ and $C_n^2V^{5/3}$ profiles in one week above the Ali observatory.

4. DISCUSSIONS AND CONCLUSIONS

Atmospheric turbulence and its seasonal variation should have strong regional characteristics. As China has a vast territory and diverse climate distributions, especially the Tibetan Plateau with complex terrain and special climate, to develop specific regional turbulence models suitable for different climatic region in China is worth in-depth and detailed study. The model method has made great progress and is statistically consistent with the measured data [Qian et al., 2020–2024], but the method itself needs to be further improved, no one model can be applied to all the sites in different regions, the model must be modified continuously, considering various influencing factors, especially in the near ground layer, to improve the calculation accuracy of optical turbulence parameters.

REFERENCES

Bougeault P, De Hui C, Fleury B. et al. Investigation of seeing by means of an atmospheric mesoscale numerical simulation[J] // ApOpt, 1995. 34(18): 3481–3488.

Businger S., Chenrubini T. Seeing clearly-the impact of atmosphere turbulence on the propagation of extroterrestrial radiation. 2011, TX: Virtualbook-worm.com Publishing Inc.: 29–34.

Cherubini T., Businger S., Lyman R. // J. Appl. Meteorological and Climatology. 2008. V. 47. 1140.

Masciadri E, Vernin J, Bougeault P. 3D mapping of optical turbulence using an atmospheric numerical model. I. A useful tool for the ground-based astronomy // A&AS. 1999a. 137: 185–202

Masciadri E, Vernin J, Bougeault P. 3D mapping of optical turbulence using an atmospheric numerical model. II. First results at Cerro Paranal[J] // A&AS. 1999b. 137: 203–216.

Qian Xuan, Yao Yongqiang et al. Statistics of cloud cover above the Ali observatory, Tibet // MNRAS. 2024. V. 529. P. 1195–1204. https://doi.org/10.1093/mnras/stae582

Qian Xuan, Yao Yongqiang et al. Optical turbulence in the atmospheric surface layer at the Ali observatory, Tibet // MNRAS. 2022. V.510. P. 5179–5186.

Qian Xuan et al. Modelling of atmospheric optical turbulence with the Weather Research and Forecasting model at the Ali observatory, Tibet // MNRAS. 2021. V. 505. P. 582–592.

Qian Xuan, Yao Yongqiang et al. Validation of the WRF model for estimating precipitable water vapor at the Ali observatory on the Tibetan Plateau // PASP. 2020a. 132:125003.

Qian Xuan, Yao Yongqiang et al. Statistics and analysis of high-altitude wind above the western Tibetan Plateau // MNRAS. 2020b. V. 498. P. 5786–5797.

Qian Xuan et al. Numberical calculations of atmospheric conditions over Tibetan Plateau by using WRF model // SPIE. 2015. V. 595. 012028 https://doi.org/10.1088/1742-6596/595/1/012028

Wang Hongshuai, Yao Yongqiang, Qian Xuan et al. The method of modeling atmospheric optical turbulence // ACTA ASTRONOMICA SINICA. 2012. V. 53, N 6. P. 527–537.